# Influence of Molecule–Surface and Molecule-Molecule Interactions on Two-Dimensional Patterns formed by Functionalised Aromatic Molecules

Sara Fortuna[*,†,‡] and Karen Johnston[*,¶]

†*Department of Chemical and Pharmaceutical Sciences, University of Trieste, Via L. Giorgieri 1, 34127 Trieste, Italy*

‡*http://www.sarafortuna.eu*

¶*Department of Chemical and Process Engineering, University of Strathclyde, James Weir Building, 75 Montrose Street, Glasgow, G1 1XJ, United Kingdom*

E-mail: s.fortuna@units.it; karen.johnston@strath.ac.uk

**Abstract**

Molecules self-assemble on surfaces forming a variety of patterns that depend on the relative strength between the intermolecular and molecule–surface interactions. In this study, the effect of the physisorption/chemisorption interplay on self-assembly is investigated using Monte Carlo simulations. The molecules are modelled as hexagonal tiles capable of assuming two distinct adsorption states, with different diffusion properties, on a hexagonal lattice. The self-assembled structures that emerge by tuning the molecule–surface and molecule–molecule interactions are systematically mapped out to develop understanding of their phase behaviour. The resulting phase diagrams will guide the engineering of novel molecules to obtain desired collective structural properties for development of innovative two-dimensional devices.

# 1. Introduction

Controlling the self-organisation of molecular adlayers is key for the development of novel two-dimensional devices, such as graphene nanostructure spintronics[1] or conjugated aromatic polymer anodes for ion batteries.[2] While the nature and strength of molecule–surface interactions control the interfacial and electronic properties of adsorbed molecules, the monolayer patterns formed are controlled by the interplay between molecule–surface and molecule–molecule interactions.[3] Therefore, in order to control the monolayer structure, one can adjust the interactions by changing the chemical properties of the molecular adlayer.

Molecular functionalisation,[4] such as the introduction of groups capable of hydrogen-bonding[5] or bulky groups,[6] is one way to adjust the molecular interactions and is well documented to affect the observed monolayer patterns.[7–9] Halogenation of molecules can heavily modify these patterns, especially for aromatic molecules. For instance pentacene is known to form two different ordered phases on Au(111) but its fluorination leads to the formation of only one single phase, in the form of ordered arrays.[10] Further examples include metallorganic molecules, such as phthalocyanines, which are known to exhibit non-

standard molecule–surface coupling that is stronger than typical physisorption but weaker than chemisorption leading to a variety of self-assembled patterns and surface reconstructions.[11,12] In this case the assemblies can be further controlled by fluorination, as observed for copper phtalocyanine patterning on Cu(100) and Cu(111).[13] The effect of fluorination on monolayer structure is also observed in benzene on metal surfaces.[14,15]

In all cases, molecular functionalisation controls the interaction parameters that drives the system towards a particular monolayer structure[3] and there are striking examples where functionalised molecules exist in two or more distinct adsorption states. Kohn-Sham density functional theory calculations have found that that on platinum heteroaromatic s-triazine can exist in multiple adsorption states,[16] and phenol[17] and benzene derivatives[18–20] exist in two states. It has been shown that on platinum the relative stability of the chemisorbed and physisorbed states of benzene molecules can be tuned by adjusting the ring functionalisation[17–20] and, hence, that the molecule–surface interaction can be used to control the structure of the self-assembled monolayer.[21]

The collective molecular behavior is affected by the interplay among different interactions and lattice models have been shown to capture experimentally observed patterns. For instance hexagonal and square lattice models[22] successfully described self-assembled molecular systems on surfaces.[21,23–27] The effect of the strength of the molecule–surface interaction was recently taken into account in a three-dimensional model for the study of triangular molecules at the solid-liquid interface[28] and in two dimensional models for the study of molecules on platinum surfaces.[21] If the adsorbed molecules are rigid, flat molecules presenting hexagonal symmetry, e.g. due to the presence of one or more fused benzene rings, the suitable symmetry for a lattice model is a hexagonal (or equivalent triangular) one.

The phase behavior of hexahalogenated molecules was previously studied analytically[29] and by Monte Carlo simulations.[21] In our previous study, we showed that hexahalogenated molecules can form either ordered, packed monolayers or disordered monolayers, depending on their preferred adsorption state.[21] Only the weakly bound (physisorbed) state allowed for

free diffusion along the surface resulting in a ordered packed state.[21] Our model gave qualitative agreement to experiment and found that benzene monolayers were disordered and halogenation (chloro- and bromination) resulted in ordering,[21] which was qualitatively similar to experimental results that fluorination increased ordering of pentacene monolayers.[10] In this paper, we generalise our model to describe molecules with hexagonal symmetry (such as hexasubstituted benzene rings[20] and larger aromatic compounds). We systematically map out the phase behaviour of self-assembled monolayers by varying the molecule–surface and intermolecular interactions, and show that these systems express a rich phase behavior. This study will enable us to understand what phases are possible, and facilitate the design of molecules and surfaces that would give a desired structure for two-dimensional devices.

## 2. Methods

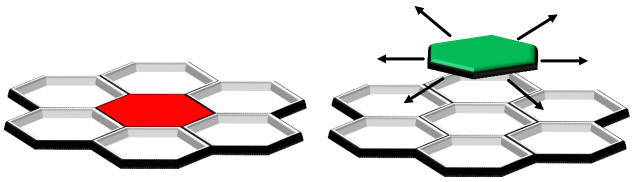

(a) chemisorbed (b) physisorbed

Figure 1: Possible molecular states. Molecules in their chemisorbed state (a) are locked in their position, while physisorbed molecules are free to diffuse on the hexagonal lattice (b).

We simulate the self-assembly of non-overlapping hexagonal molecules on a hexagonal lattice in the NVT ensemble. On the lattice each molecule $i$ can be in one of two possible adsorption states $s_i$ (as in Fig. 1): chemisorbed ($s_i$ = chem) or physisorbed ($s_i$ = phys) . Each lattice site can be occupied by only one molecule.

Two adjacent molecules, $i$ and $j$, interact with each other via the interaction parameter, $E_{ij}^{\text{side}}$. When both molecules are in different adsorption states i.e. when $s_i = s_j$, it is assumed that the interaction is negligible and $E_{ij}^{\text{side}} = 0$. Molecules interact with the surface via the interaction parameter $E_{\text{ads}}^{\text{phys}}$ when physisorbed, and $E_{\text{ads}}^{\text{chem}}$ when chemisorbed. The

Hamiltonian of the system is:

$$H = \sum_i E_{\text{ads}}^{s_i} + \frac{1}{2} \sum_{i,j} E_{ij}^{s_i,s_j} \quad \text{with} \quad i \neq j \tag{1}$$

where

$$E_{ij}^{s_i,s_j} = \begin{cases} E_{ij}^{\text{side}} & \text{if } s_i = s_j \\ 0 & \text{otherwise} \end{cases} \tag{2}$$

and $E_{\text{ads}}^{s_i}$ is the adsorption energy for molecule $i$, which can be in either the physisorbed ($E_{\text{ads}}^{s_i} = E_{\text{ads}}^{\text{phys}}$) or chemisorbed states ($E_{\text{ads}}^{s_i} = E_{\text{ads}}^{\text{chem}}$). The first summation is taken over all molecules and the second summation is only over adjacent molecules. All energies are in units of $k_{\text{B}}T$, where $k_{\text{B}}$ is the Boltzmann constant.

At each simulation step a molecule is selected at random and either a chemisorbed/physisorbed transition occurs or a translation to the next lattice site is attempted. Only one move can be attempted at each simulation step. Only physisorbed molecules can translate to adjacent sites. If a molecule is chemisorbed only a transition to a physisorbed state is possible. All the attempted moves are accepted or rejected following the Metropolis acceptance probability.[30] We do not account for rotations, therefore $E_{ij}^{\text{side}}$ is constant for all the molecular orientations.

The system is composed of 1000 molecules interacting via the Hamiltonian in Eq. (1) on a $50 \times 50$ hexagonal lattice with periodic boundary conditions, corresponding to a coverage of 0.4. To verify the effect of the coverage, selected parameter combinations were also run with 972 molecules on a $54 \times 54$ lattice corresponding to a coverage of 0.33.

A chain of 400 simulations is built, with each simulation consisting of 5,000,000 equilibration steps followed by 5,000,000 production steps. Every chain starts at $0.4k_{\text{B}}T$ and every successive simulation is run by decreasing the temperature by $\Delta k_{\text{B}}T = 0.002$ and using the last configuration of the former simulation as starting configuration. The low temperature configurations are then heated back to $0.4k_{\text{B}}T$ following the same protocol. Each simulation chain is repeated 10 times. Averages are calculated over the production steps of the 10

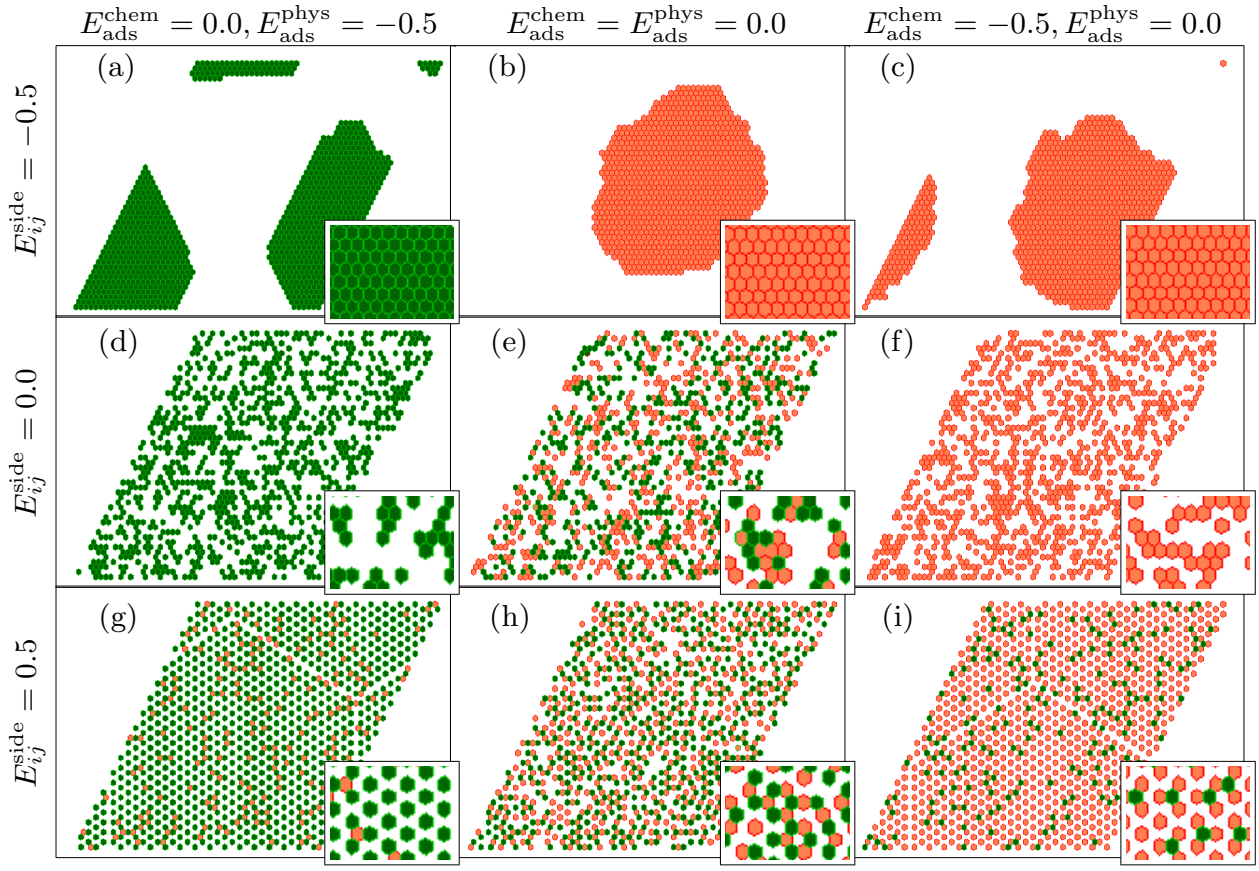


Figure 2: Patterns formed at $k_{\rm B}T = 0.002$. Insets show an enlarged detail of each snapshot. Physisorbed (chemisorbed) molecules are shown as green (orange).

simulations run with the same parameter set. No hysteresis effects were observed, therefore, in the next section we will discuss only the results obtained upon cooling.

We generalise our former study[21] by exploring a larger parameter space $E_{\rm ads}^{\rm phys} = [-0.5, 0.0]$, $E_{\rm ads}^{\rm chem} = [-0.5, 0.0]$ and $E_{ij}^{\rm side} = [-0.5, 0.5]$. As we are interested in exploring trends, and keeping in mind that all the energy parameters are in units of $k_{\rm B}T$ and can therefore be rescaled, only their ratio is important. Each parameter is chosen among 0, $\pm 0.001$, $\pm 0.005$, $\pm 0.01$, $\pm 0.05$, $\pm 0.1$,$\pm 0.5$. By combining $E_{\rm ads}^{\rm phys}$, $E_{\rm ads}^{\rm chem}$, $E_{ij}^{\rm side}$ we obtain 637 systems each ruled by a different parameter set.

# 3. Results and Discussion

In the following, we first look at low temperature limiting cases. Then we look at the details of the structural transitions encountered to produce the observed patterns. The behaviour of the system is described by the heat capacity at constant volume

$$C_V = \frac{(\Delta E)^2}{k_{\mathrm{B}} T^2},$$

and several different order parameters:

(i) the fraction of physisorbed molecules, $\chi_{\mathrm{phys}}$,

(ii) the total number of neighbors of each molecule, $N^{\mathrm{neigh}}$,

(iii) the number of chemisorbed neighbors of each chemisorbed molecule, $N^{\mathrm{cc}}$,

(iv) the number of physisorbed neighbors of each physisorbed molecule, $N^{\mathrm{pp}}$,

(v) and the number of unlike neighbors

$$N^{\mathrm{pc}} = N^{\mathrm{cp}} = N^{\mathrm{neigh}} - N^{\mathrm{pp}} - N^{\mathrm{cc}}$$

The peaks in the running standard deviations of these order parameters enables us to further locate the locus of structural transitions. Finally, after characterising the observed defects on the self-assembled structures, we collect our results in a number of phase diagrams associated with the choice of parameters.

## 3.1 Low temperature phases

By first looking at few limiting cases, a number of low-temperature ($k_{\mathrm{B}} T = 0.002$) patterns are observed (Fig. 2).

Strong, attractive molecule–molecule interactions with $E_{ij}^{\text{side}} = -0.5$ lead to packed patterns (Fig. 2a-c). The molecules can be all physisorbed, for instance when the chemisorbed interaction is switched off, as shown in Fig. 2a, or all chemisorbed when the physisorption interaction is switched off, as shown in Fig. 2c. When both chemisorption and physisorption interactions are set to zero, a single chemisorbed cluster is observed (Fig. 2b). This chemisorbed configuration arises from the fact that molecules are not mobile in the chemisorbed state while they can freely diffuse in the physisorbed state. When a first chemisorbed cluster forms, further molecules from the physisorbed state can add to it and then be locked in their position favouring a large packed chemisorbed pattern at low temperature.

When the molecule–molecule interaction is switched off, i.e. $E_{ij}^{\text{side}} = 0.0$, the system does not pack, as shown in Figs. 2d-f. The system freezes in a disordered state whose adsorption state of the frozen molecules depends on the relative strength of the adsorption energies (Fig. 3). When $E_{\text{ads}}^{\text{chem}} = E_{\text{ads}}^{\text{phys}}$ half of the molecules are chemisorbed, and the rest are physisorbed (Fig. 2e). When $E_{\text{ads}}^{\text{phys}} \ll E_{\text{ads}}^{\text{chem}} = 0.0$ they are all physisorbed (Fig. 2d) when $E_{\text{ads}}^{\text{chem}} \ll E_{\text{ads}}^{\text{phys}} = 0$ they are all chemisorbed (Fig. 2f). In the case when $E_{\text{ads}}^{\text{phys}}$ and $E_{\text{ads}}^{\text{chem}}$ are both negative but much weaker (closer to zero) the number of physisorbed/chemisorbed molecules depends on their respective interaction strength. For instance, when $E_{\text{ads}}^{\text{chem}} = 0.001$ and $E_{\text{ads}}^{\text{phys}} = 0.01$ only 40% of the molecules are chemisorbed whereas when $E_{\text{ads}}^{\text{chem}} = 0.01$ and $E_{\text{ads}}^{\text{phys}} = 0.001$ then 60% are chemisorbed (Fig. 3).

In the case of repulsive intermolecular interactions (for instance when $E_{ij}^{\text{side}} = 0.5$) we would expect molecules to avoid occupying adjacent lattice sites. When the coverage is greater than $\frac{1}{3}$ (as is the case when the coverage is 0.4) we observe a number of strategies to escape higher energy configurations. Depending on the physisorption and chemisorption strength we observe the formation of:

- an ordered layer of physisorbed molecules with dislocations and defects in the form of chemisorbed molecules when $E_{\text{ads}}^{\text{phys}} \ll E_{\text{ads}}^{\text{chem}} = 0.0$ (Fig. 2g),

- a frozen state composed of branched chains and ribbons of alternating physisorbed/chemisorbed

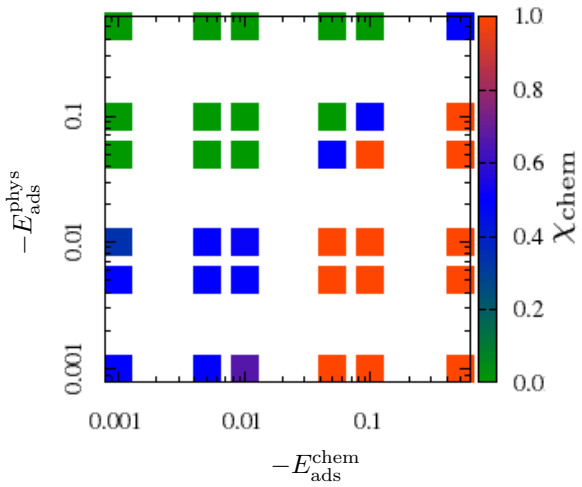


Figure 3: Fraction of chemisorbed molecules as a function of $E_{\rm ads}^{\rm phys}$ and $E_{\rm ads}^{\rm chem}$ for $E_{ij}^{\rm side} = 0.0$ at $k_{\rm B}T = 0.002$.

molecules when $E_{\rm ads}^{\rm phys} = E_{\rm ads}^{\rm chem} = 0.0$ (Fig. 2h), and

- an ordered layer of chemisorbed molecules with dislocations and defects in the form of physisorbed molecules when $E_{\rm ads}^{\rm chem} \ll E_{\rm ads}^{\rm phys} = 0.0$ (Fig. 2i).

If the coverage is below or equal to 0.33, we might expect to observe complete order. Interestingly, when $E_{\rm ads}^{\rm phys} \ll E_{\rm ads}^{\rm chem} = 0.0$ (Fig. 4a) complete order is not achieved and defects in the form of vacancies or insertions are present. It is the non-mobile chemisorption state that causes these defects. Chemisorbed molecules would have to first become physisorbed in order to migrate to a new adsorption site, but this process is hindered due to repulsive intermolecular interactions between molecules in the same adsorption state. When $E_{\rm ads}^{\rm chem} \ll E_{\rm ads}^{\rm phys} = 0.0$ (Fig. 4b), physisorbed molecules at defect sites can escape and freely diffuse to fill all the vacancies enabling complete order to be reached.

The formation of defects can be better understood by observing their occurrence at fixed values of adsorption energies along increasing values of $E_{ij}^{\rm side}$ (Fig. 5). Defects appear in different forms, depending on the interplay among interactions. For instance, at $E_{\rm ads}^{\rm chem} = -0.05$, $E_{\rm ads}^{\rm phys} = -0.01$, and going from $E_{ij}^{\rm side} = -0.05$ to 0.00 first the packed structures become fragmented as the side-side interactions weaken with respect to $E_{\rm ads}^{\rm chem}$ (Fig. 5, top

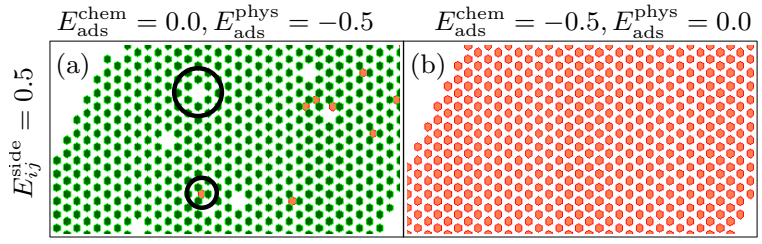


Figure 4: Patterns formed at $k_{\rm B}T = 0.002$. Physisorbed molecules (green), chemisorbed molecules (orange). At coverage 0.33. Structural defects are highlightd by black circles.

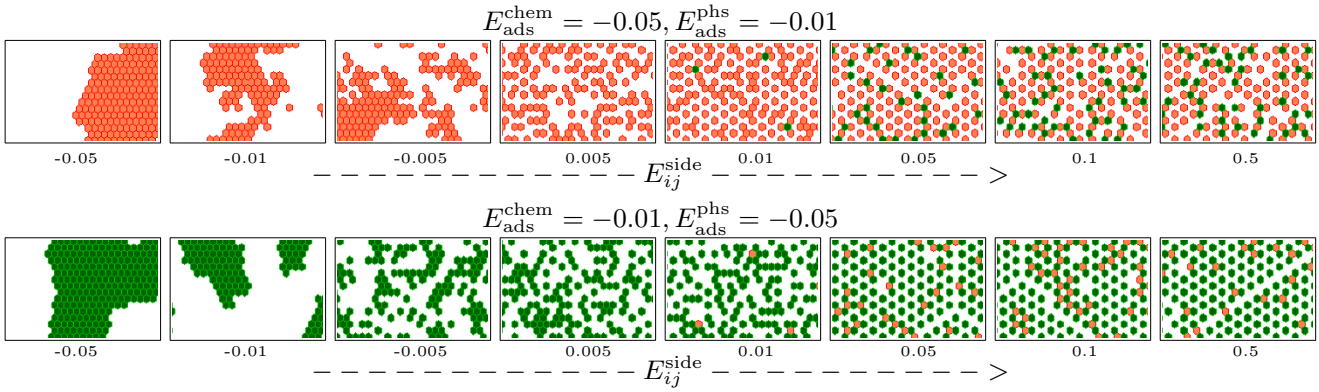


Figure 5: Defect formation in the patterns formed at fixed $E_{\rm ads}^{\rm chem}$ and $E_{\rm ads}^{\rm phys}$ at $0.002 k_{\rm B}T$. Physisorbed (chemisorbed) molecules are shown in green (orange).

panels). When the side interactions are close to zero the structure is completely fragmented. Fragmentation persists at 0.005 and defects of physisorbed molecules emerge at more positive $E_{ij}^{\rm side}$ (0.01). The more repulsive the intermolecular interaction, the higher the number of physisorption defects. When $E_{ij}^{\rm side} \sim (-E_{\rm ads}^{\rm chem})$ a new ordered state emerges with grain boundary defects. When $E_{ij}^{\rm side} \geq (-E_{\rm ads}^{\rm chem})$ the grain boundaries increase and the patterns again appear fragmented. A similar observation applies for the case in which $E_{\rm ads}^{\rm chem} = -0.01$ and $E_{\rm ads}^{\rm phys} = -0.05$ (Fig. 5, bottom panels). However, when $E_{ij}^{\rm side} \geq (-E_{\rm ads}^{\rm phys})$, the pattern remains ordered with grain boundary and chemisorption defects.

## 3.2 Phase transitions

In this section we investigate the structures that emerge at different temperatures. By looking at the phase behavior along $k_{\rm B}T$, the peaks in the heat capacity enable the identification of

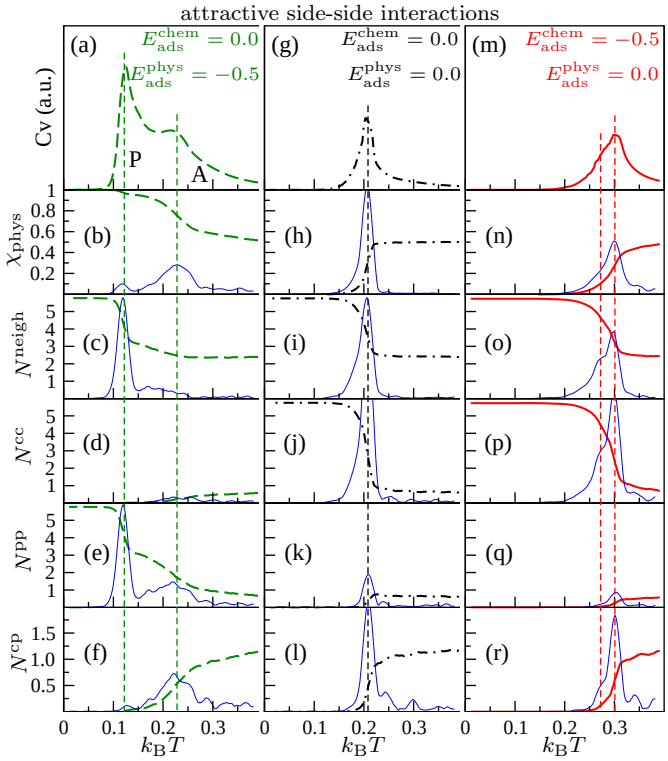


Figure 6: Self-assembly for attractive intermolecular interactions with $E_{ij}^{\rm side} = -0.5$, corresponding to the low temperature phases in Fig. 2a-c. The top panels show the variation of $C_V$ in arbitrary units (a.u.) with temperature. The lower panels show running averages (calculated over 10 points) of order parameters with temperature. Also indicated in blue solid lines are the respective running standard deviations (calculated over 10 points) and 10× magnified.

the sequence of structural transitions that lead to the observed low temperature patterns. The structures encountered can be further characterised by a number of order parameters defined earlier: $\chi_{\rm phys}$, $N^{\rm neigh}$, $N^{\rm cc}$, $N^{\rm pp}$, and $N^{\rm cp}$ (Fig. 6-8).

**3.2.1 Attractive intermolecular interactions** For attractive intermolecular interactions with $E_{\rm ads}^{\rm chem} = 0.0$ and $E_{\rm ads}^{\rm phys} = E_{ij}^{\rm side} = -0.5$, leading to the zero temperature physisorbed packed pattern of Fig. 2a, two major transitions can be observed (Fig. 6a-f). The first is a high temperature physisorption/chemisorption transition characterised by a peak in $C_V$ (Fig. 6a), and associated with a rapid variation in $\chi_{\rm phys}$ (Fig. 6b), no large variations in $N^{\rm neigh}$ (Fig. 6c) and $N^{\rm cc}$ (Fig. 6d), and a smooth variation in $N^{\rm pp}$(Fig. 6e) and $N^{\rm cp}$ (Fig. 6f) at $0.23k_{\rm B}T$. This $C_V$ peak appears as shoulder on the main $C_V$ peak at $0.12k_{\rm B}T$ (Fig. 6a),

which is associated with a rapid change in $N^{\mathrm{neigh}}$ and $N^{\mathrm{pp}}$ (Fig. 6c,e). The low temperature value of $N^{\mathrm{pp}}$, which is close to its maximum value of 6, indicates the packing of the system in a physisorbed state.

The case leading to the chemisorbed pattern of Fig. 2b follows a different route (Fig. 6g-l). In this case, the molecules do not interact with the surface ($E_{\mathrm{ads}}^{\mathrm{chem}} = E_{\mathrm{ads}}^{\mathrm{phys}} = 0.0$) but have attractive intermolecular interactions between molecules in the same adsorption state ($E_{ij}^{\mathrm{side}} = -0.5$). Only one sharp $C_V$ peak is present and physisorption/chemisorption and packing transitions both take place at the same temperature, as shown in Fig. 6 g-l. Interestingly, even though there is no energetic preference with respect to the adsorption state, the molecules pack in a chemisorbed state, which is an effect of their arrested translational mobility in that phase.

When $E_{\mathrm{ads}}^{\mathrm{phys}} = 0.0$ and $E_{\mathrm{ads}}^{\mathrm{chem}} = E_{ij}^{\mathrm{side}} = -0.5$ (Fig. 6m-r), then $C_V$ exhibits a main peak and a weak shoulder as shown in Fig. 6m. The shoulder is the low temperature packing peak, now at $0.27 k_{\mathrm{B}}T$. The higher temperature main peak at $0.30 k_{\mathrm{B}}T$ is the physisorption/chemisorption transition. Here all the order parameters sharply decreases (Fig. 6n-r) with only $N^{\mathrm{pp}}$ going to zero (Fig. 6q), while $\chi_{\mathrm{phys}}$ (Fig. 6n) and $N^{\mathrm{cp}}$ (Fig. 6r) continues to decrease and $N^{\mathrm{neigh}}$ (Fig. 6o) and $N^{\mathrm{cc}}$ (Fig. 6p) continues to increase at both temperatures. The low temperature structure is once again a chemisorbed packed pattern (Fig. 2c).

**3.2.2 Zero intermolecular interactions** When the intermolecular interactions are set to zero ($E_{ij}^{\mathrm{side}} = 0$) leading to the disordered patterns of Fig. 2d-f, there appears to be a single structural transition only when the molecule–surface interaction is active (Fig. 7a-r).

When $E_{\mathrm{ads}}^{\mathrm{chem}} = 0.0$ and $E_{\mathrm{ads}}^{\mathrm{phys}} = -0.5$ there is a large peak in $C_V$ (Fig. 7a). This is a physisorption/chemisorption transition leading to all molecules in their favoured physisorbed state (Fig. 7b). Packing, of course, does not take place and $N^{\mathrm{neigh}}$ is constant with temperature (Fig. 7c). As the temperature decreases, the number of like neighbors in the unfavoured adsorption state decreases (Fig. 7d) while the number of like neighbours increases in the

favoured state (Fig. 7e). Also the number of unlike neighbors drops to zero (Fig. 7f).

As expected, when all the interactions are set to zero, no transition is observed, all the order parameters are constant along the temperature (Fig. 7g-l) and the system stays disordered.

On the other hand, in the scenario in which $E_{\mathrm{ads}}^{\mathrm{chem}} = -0.5$ and $E_{\mathrm{ads}}^{\mathrm{phys}} = 0.0$ the observed large peak in the $C_V$ (Fig. 7m) is once again associated with a physisorption/chemisorption transition leading to all molecules in their favoured adsorption state, which in this case is chemisorbed (Fig. 7n). As the molecules do not interact with each other, packing still does not take place as highlighted by the constant values of $N^{\mathrm{neigh}}$ (Fig. 7o). As the temperature decreases the number of like neighbors in the favoured adsorption state increases (Fig. 7p) while the number of like neighbours decreases in the unfavoured state (Fig. 7q), and the number of unlike neighbors drops to zero (Fig. 7r).

**3.2.3 Repulsive intermolecular interactions** Finally, we present the self-assembly when the intermolecular interactions are repulsive ($E_{ij}^{\mathrm{side}} = 0.5$, Fig. 2g-i) and molecules occupying adjacent lattice sites will attempt to minimise repulsive interactions by minimising the number of neighbors in the same adsorption state (Fig. 8a-r). When the physisorption state is energetically favorable, for instance with $E_{\mathrm{ads}}^{\mathrm{chem}} = 0.0$ and $E_{\mathrm{ads}}^{\mathrm{phys}} = -0.5$, decreasing the temperature first shows a shoulder on the main $C_V$ peak at $\approx 0.12 k_{\mathrm{B}}T$ (Fig. 8a) with a minimal variation in $\chi_{\mathrm{phys}}$ (Fig. 8b), the onset of $N^{\mathrm{neigh}}$ drop (Fig. 8c), and a slow decrease in $N^{\mathrm{cc}}$ (Fig. 8d).

The main peak in $C_V$ at lower temperature of $\approx 0.06 k_{\mathrm{B}}T$ (Fig. 8a) corresponds to a more significant physisorption/chemisorption transition (Fig. 8b). There is a decrease in the total number of neighbors, $N^{\mathrm{pp}}$ (Fig. 8e). Below this temperature $N^{\mathrm{cc}}$ (Fig. 8d) and $N^{\mathrm{pp}}$ (Fig. 8e) fall to zero leaving only unlike neighbours (Fig. 8f).

When both physisorbed and chemisorbed adsorption energies are zero, there is only one peak in $C_V$ (Fig. 8g), not associated with any variation in $\chi_{\mathrm{phys}}$ (Fig. 8h) which corresponds

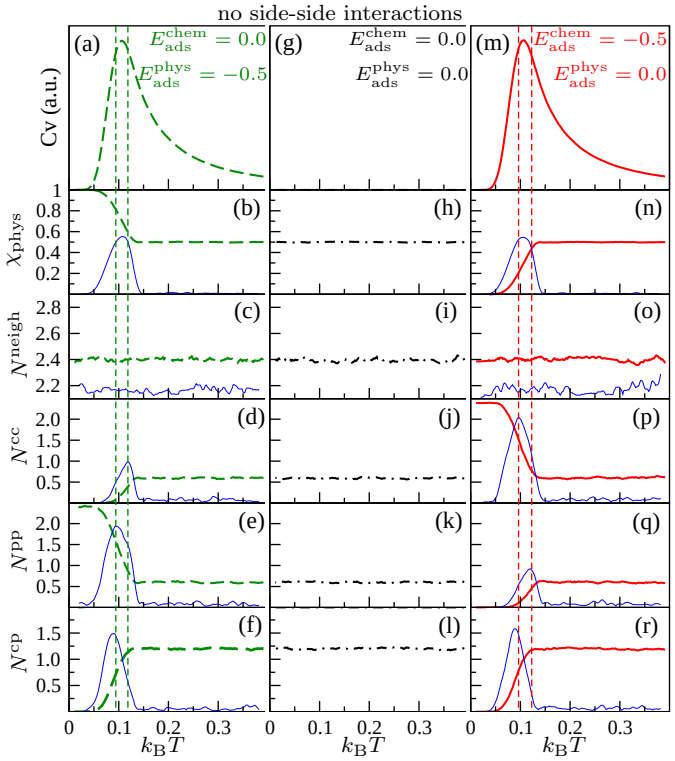


Figure 7: Self-assembly for zero intermolecular interactions with $E_{ij}^{side} = 0.0$, corresponding to the low temperature phases in Fig. 2 d-f. The top panels show the variation of $C_V$ in arbitrary units (a.u.) with temperature. The lower panels show running averages (calculated over 10 points) of order parameters with temperature. Also indicated in blue solid lines are the respective running standard deviations (calculated over 10 points) and 10× magnified.

to a decrease in $N^{neigh}$ which goes to 0.16 (Fig. 8i) and in $N^{cc}$ (Fig. 8j) and $N^{pp}$ (Fig. 8k) both going to zero. A slight increase in unlike neighbours $N^{cp}$ is also observed (Fig. 8l). The order parameter standard deviations are observed to be double peaks (Fig. 8i-l). In this case, the low temperature structure has chains of alternating physisorbed and chemisorbed molecules (Fig. 2h).

Two unresolved peaks on the $C_V$ are also observed when the most favourable adsorption state is chemisorbed, for instance with $E_{ads}^{chem} = -0.5$ and $E_{ads}^{phys} = 0.0$ (Fig. 8m). A drop in $\chi_{phys}$ (Fig. 8n) is associated only with the low temperature main transition at $0.11k_BT$, while $N^{neigh}$ (Fig. 8o) and $N^{cc}$ (Fig. 8p) tend to drop at both the temperatures identified by the $C_V$ peaks. $N^{pp}$ is minimised at $0.11k_BT$ (Fig. 8q) while the onset of $N^{cp}$ drop is observed at the same temperature (Fig. 8r).

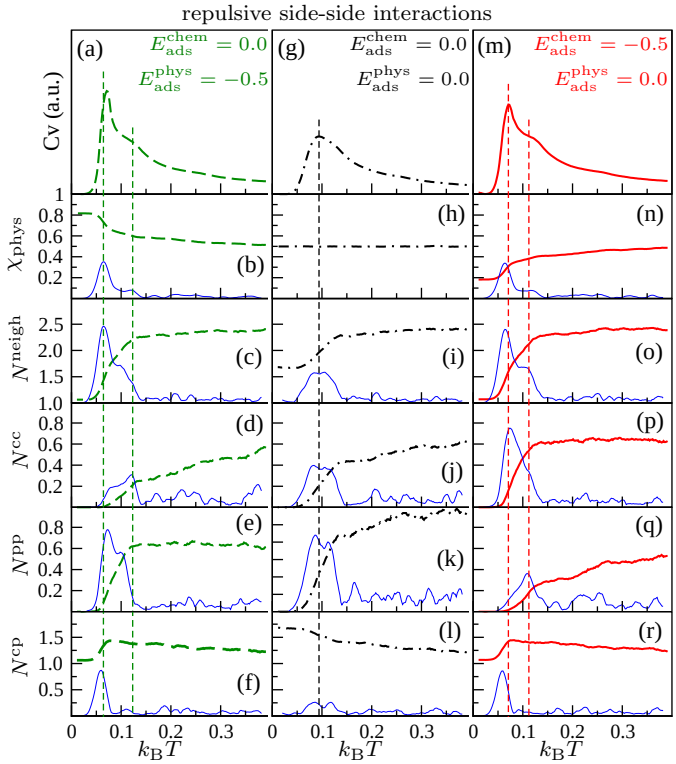


Figure 8: Self-assembly for repulsive intermolecular interactions with $E_{ij}^{\rm side} = 0.5$, corresponding to the low temperature phases in Fig. 2g-i. The top panels show the variation of $C_V$ in arbitrary units (a.u.) with temperature. The lower panels show running averages (calculated over 10 points) of order parameters with temperature. Also indicated in blue solid lines are the respective running standard deviations (calculated over 10 points) and 10× magnified.

## 3.3 Phase diagrams

The observed phases and defect patterns enable the entire configurational space to be characterised, and in Fig. 9 the observed low temperature patterns are schematised into a series of two-dimensional $E_{\rm ads}^{\rm chem}$ vs $E_{\rm ads}^{\rm phys}$ phase diagrams. Each phase diagram is characterised by a different intermolecular interaction strength $E_{ij}^{\rm side}$ (for molecules are in the same adsorption state, see Eq. 2). In these plots an inverse logarithmic scale has been employed for clarity.

Attractive intermolecular interactions that are stronger or equal to the physisorption or chemisorption interactions always lead to packing in the form of a large ordered cluster. In the majority of cases all molecules are chemisorbed, which is due to no translation in the chemisorbed state. Only when $-E_{\rm ads}^{\rm phys} \geq -E_{ij}^{\rm side}$ and $-E_{\rm ads}^{\rm phys} > -E_{\rm ads}^{\rm chem}$ we observe that all

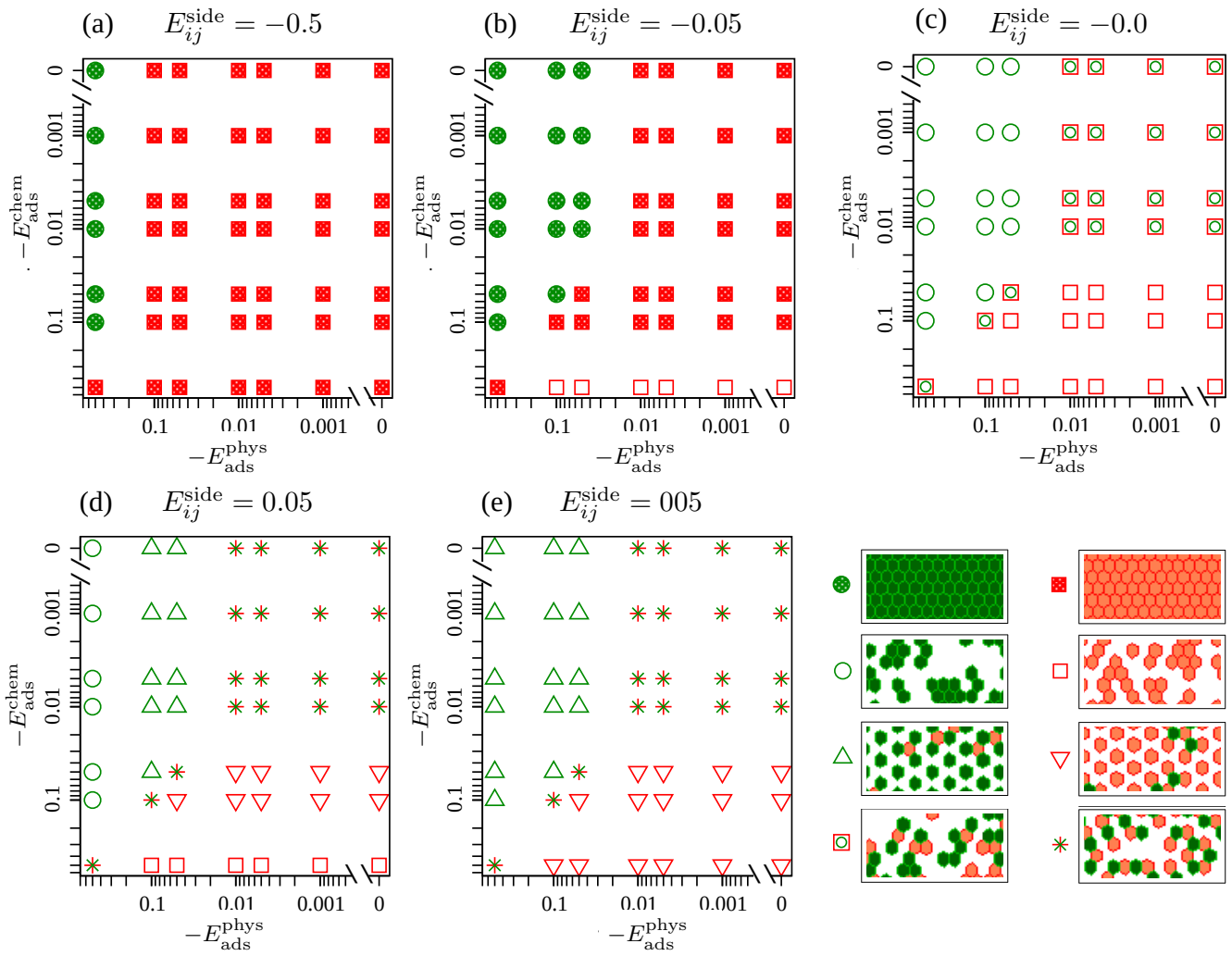


Figure 9: Phase behavior at fixed $E_{ij}^{\rm side}$ at $0.002 k_{\rm B}T$ for different physisorbed and chemisorbed interactions. Physisorbed (chemisorbed) molecules are shown in green (orange).

molecules are physisorbed. In the particular cases explored in Fig. 9a this is observed only when $E_{\rm ads}^{\rm phys} = -0.5$ and $E_{\rm ads}^{\rm chem} \leq -0.1$.

When the intermolecular interactions are decreased by a factor of ten (i.e. $E_{ij}^{\rm side} = -0.05$, Fig. 9b) we again observe that the patterns are physisorbed when $-E_{\rm ads}^{\rm phys} \geq -E_{ij}^{\rm side}$ and $-E_{\rm ads}^{\rm phys} > -E_{\rm ads}^{\rm chem}$, and chemisorbed otherwise. While in most cases large islands with irregular boundaries are observed, when $-E_{\rm ads}^{\rm chem} = 0.5$ and $-E_{\rm ads}^{\rm phys} \leq 0.1$ the chemisorbed molecules tend to form single molecule chains and small clusters. Dimers, trimers, and isolated molecules are also observed.

When the intermolecular interactions are zero (Fig. 9c), the patterns are driven only by the interplay between the adsorption energies. The phase diagram is clearly symmetrical and dominated by the presence of chains and small clusters. These are all physisorbed when $-E_{\text{ads}}^{\text{phys}} > -E_{\text{ads}}^{\text{chem}}$ and $-E_{\text{ads}}^{\text{phys}} \geq 0.01$, and chemisorbed when $-E_{\text{ads}}^{\text{chem}} \geq -E_{\text{ads}}^{\text{phys}}$ and $-E_{\text{ads}}^{\text{chem}} \geq 0.01$. In the residual portion of the phase diagram molecules are randomly distributed among the two states. The ratio of molecules in each adsorption state depends on the strength of $E_{\text{ads}}^{\text{phys}}$ and $E_{\text{ads}}^{\text{chem}}$ as already discussed in the former section and shown in Fig. 3.

In the presence of repulsive interactions between molecules, no packed patterns are observed (Fig. 9d-e). When $E_{\text{ads}}^{\text{phys}} = E_{\text{ads}}^{\text{chem}}$ or $-E_{\text{ads}}^{\text{phys}}$ and $-E_{\text{ads}}^{\text{chem}}$ are $\leq 0.01$, the pattern exhibits physisorbed and chemisorbed molecules, with molecules arranged in small clusters or chains. When the chemisorption (physisorption) interaction is stronger, the molecules transition to the preferred adsorption state, forcing the molecules to move apart to minimise the repulsive intermolecular interactions. This forms an orderly state with molecules in the preferred adsorption state in alternating sites and molecules in the other state in randomly distributed sites. This effect arises since only molecules in the same adsorption state are repelled.

The only difference in the phase diagrams of strong and weak repulsive intermolecular interactions occurs when there is strong physisorption and weak chemisorption, or vice versa. For example, weak intermolecular interactions $E_{ij}^{\text{side}} = 0.05$, coupled with strong physisorption $E_{\text{ads}}^{\text{phys}} = -0.5$ and weak chemisorption $E_{\text{ads}}^{\text{chem}} \leq -0.1$ give rise to the presence of physisorbed chains and small clusters. These are instead all chemisorbed when $E_{\text{ads}}^{\text{phys}} \leq -0.1$ and $E_{\text{ads}}^{\text{chem}} = -0.5$ (Fig. 9d).

# 4. Conclusions

In this paper we employed a hexagonal lattice model[21] to simulate the phase behaviour of gas phase deposition of generic molecules with $C_6$ symmetry, such as benzene derivatives, on metallic surfaces. The molecules could express two distinct adsorption states: chemisorbed and physisorbed, and had variable intermolecular interactions. Molecules were allowed to freely to diffuse only in the physisorbed state, but were locked in their position when chemisorbed to mimic a strong site preference. Monte Carlo simulations were used to explore the parameter space and the emerging structures were characterised and used to map out resulting phase diagrams.

Phase behavior as a function of temperature was explored and two main types of transitions were observed, namely, change of adsorption state, and packing/ordering. For attractive intermolecular interactions, the high temperature transition is a change of adsorption state and the low temperature transition is packing. When molecule–surface interactions are weak, the two transitions overlap. When there are no intermolecular interactions, the system undergoes only a single transition, which is a change of adsorption state, and the system remains disordered. For repulsive intermolecular interactions there are two transitions, which are change of adsorption state and ordering to minimise the number of neighbours. However, these transitions are not well resolved with respect to temperature.

The overall phase behavior at low temperature reflects these observations. For attractive intermolecular interactions, regardless of the favoured adsorption state, molecules tend to lock into a chemisorbed packed state. All-physisorbed systems are only favoured when the mobile physisorbed state interacts with the surface much more strongly than the chemisorbed state. When molecules do not interact with each other, no packing is observed and the low temperature patterns are ruled by the ratio between the two adsorption strengths. For strongly repulsive intermolecular interactions a long range order for the preferred adsorption state is observed. When the physisorbed state is stronger than the chemisorbed state defects occur, even at low coverage, due to the lack of mobility of chemisorbed molecules.

The employed model has two main approximations. The first is that the lattice approximates the surface by limiting the adsorption sites to the hollow site and neglects bridge and top sites. However, when molecules adsorb on an fcc (111) surface, it can be that the preferred adsorption site is different for the chemisorption and physisorption states of different molecules. A future direction for model development would be to use two (or more) interpenetrating lattices and allow for multiple adsorption sites. The second approximation is the representation of the intermolecular interactions. The number of parameters for the side-side interactions increases significantly for lower symmetry molecules and by different side-side interactions between different adsorption states. While steps in this direction are being made, the current model is applicable to molecules with six-fold symmetry and assumes that molecules in different adsorption states do not interact.

This model demonstrating that a variety of self-assembled structure can be obtained will aid the design of self-assembly of molecular monolayers on metallic surfaces. To obtain a specific monolayer pattern molecules can be functionalised to obtain the desired intermolecular and surface interactions leading to directed assembly of the monolayer. In future work, the model can be modified to account for additional interactions and more complex molecular systems and be used to design a monolayer structure for two-dimensional device applications.

## Acknowledgements

We gratefully acknowledge the Academia Nazionale dei Lincei and the Royal Society of Edinburgh for financial support.

## References

(1) Ruffieux, P.; Wang, S.; Yang, B.; Sánchez-Sánchez, C.; Liu, J.; Dienel, T.; Talirz, L.; Shinde, P.; Pignedoli, C. A.; Passerone, D. et al. On-surface synthesis of graphene nanoribbons with zigzag edge topology. *Nature* **2016**, *531*, 489.

(2) Liu, W.; Luo, X.; Bao, Y.; Liu, Y. P.; Ning, G.-H.; Abdelwahab, I.; Li, L.; Nai, C. T.; Hu, Z. G.; Zhao, D. et al. A two-dimensional conjugated aromatic polymer via C–C coupling reaction. *Nat. Chem.* **2017**, *9*, 563.

(3) Whitelam, S. Examples of molecular self-assembly at surfaces. *Adv. Mater.* **2015**, *27*, 5720–5725.

(4) Bouju, X.; Mattioli, C.; Franc, G.; Pujol, A.; Gourdon, A. Bicomponent supramolecular architectures at the vacuum–solid interface. *Chem. Rev.* **2017**, *117*, 1407–1444.

(5) Kühnle, A. self-assembly of organic molecules at metal surfaces. *Curr. Opin. Colloid Interf. Sci.* **2009**, *14*, 157–168.

(6) Szabelski, P.; Nieckarz, D.; Rżysko, W. Influence of molecular shape and interaction anisotropy on the self-assembly of tripod building blocks on solid surfaces. *Coll. Surf. A* **2017**, *532*, 522–529.

(7) Barth, J. V.; Costantini, G.; Kern, K. Engineering atomic and molecular nanostructures at surfaces. *Nature* **2005**, *437*, 671–679.

(8) Barth, J. V. Molecular architectonic on metal surfaces. *Ann. Rev. Phys. Chem.* **2007**, *58*, 375–407.

(9) Maurer, R. J.; Ruiz, V. G.; Camarillo-Cisneros, J.; Liu, W.; Ferri, N.; Reuter, K.; Tkatchenko, A. Adsorption structures and energetics of molecules on metal surfaces: Bridging experiment and theory. *Prog. Surf. Sci.* **2016**, *91*, 72–100.

(10) Wong, S. L.; Huang, H.; Huang, Y. L.; Wang, Y. Z.; Gao, X. Y.; Suzuki, T.; Chen, W.; Wee, A. T. S. Effect of fluorination on the olecular packing of perfluoropentacene and pentacene ultrathin films on Ag (111). *J. Phys. Chem. C* **2010**, *114*, 9356–9361.

(11) Fortuna, S.; Gargiani, P.; Betti, M. G.; Mariani, C.; Calzolari, A.; Modesti, S.; Fabris, S.

Molecule-driven substrate reconstruction in the two-dimensional self-organization of Fe-phthalocyanines on Au (110). *J. Phys. Chem. C* **2012**, *116*, 6251–6258.

(12) Betti, M. G.; Gargiani, P.; Mariani, C.; Biagi, R.; Fujii, J.; Rossi, G.; Resta, A.; Fabris, S.; Fortuna, S.; Torrelles, X. et al. Structural phases of ordered FePc-nanochains self-assembled on Au (110). *Langmuir* **2012**, *28*, 13232–13240.

(13) de Oteyza, D. G.; El-Sayed, A.; Garcia-Lastra, J. M.; Goiri, E.; Krauss, T. N.; Turak, A.; Barrena, E.; Dosch, H.; Zegenhagen, J.; Rubio, A. et al. Copper-phthalocyanine based metal-organic interfaces: The effect of fluorination, the substrate, and its symmetry. *J. Chem. Phys.* **2010**, *133*, 214703.

(14) Wander, A.; Held, G.; Hwang, R.; Blackman, G.; Xu, M.; de Andres, P.; Hove, M. V.; Somorjai, G. A diffuse {LEED} study of the adsorption structure of disordered benzene on Pt(111). *Surf. Sci.* **1991**, *249*, 21 – 34.

(15) Yau, S.-L.; Kim, Y.-G.; Itaya, K. In situ scanning tunneling microscopy of benzene adsorbed on Rh(111) and Pt(111) in HF solution. *J. Am. Chem. Soc.* **1996**, *118*, 7795–7803.

(16) Filimonov, S. N.; Liu, W.; Tkatchenko, A. Molecular seesaw: Intricate dynamics and versatile chemistry of heteroaromatics on metal surfaces. *J. Phys. Chem. Lett* **2017**, *8*, 1235–1240.

(17) Peköz, R.; Donadio, D. Effect of van der Waals interactions on the chemisorption and physisorption of phenol and phenoxy on metal surfaces. *J. Chem. Phys.* **2016**, *145*, 104701.

(18) Liu, W.; Filimonov, S. N.; Carrasco, J.; Tkatchenko, A. Molecular switches from benzene derivatives adsorbed on metal surfaces. *Nat. Commun.* **2013**, *4*, 2569.

(19) Peköz, R.; Johnston, K.; Donadio, D. Tuning the adsorption of aromatic molecules on platinum via halogenation. *J. Phys. Chem. C* **2014**, *118*, 6235–6241.

(20) Johnston, K.; Pekoz, R.; Donadio, D. Adsorption of polyiodobenzene molecules on the Pt (111) surface using van der Waals density functional theory. *Surf. Sci.* **2016**, *644*, 113–121.

(21) Fortuna, S.; Cheung, D. L.; Johnston, K. Phase behaviour of self-assembled monolayers controlled by tuning physisorbed and chemisorbed states: A lattice-model view. *J. Chem. Phys.* **2016**, *144*, 134707.

(22) Gorbunov, V.; Akimenko, S.; Myshlyavtsev, A. Adsorption thermodynamics of cross-shaped molecules with one attractive arm on random heterogeneous square lattice. *Adsorption* **2016**, *22*, 621–630.

(23) Fortuna, S.; Cheung, D. L.; Troisi, A. Hexagonal lattice model of the patterns formed by hydrogen-bonded molecules on the surface. *J. Phys. Chem. B* **2010**, *114*, 1849–1858.

(24) Joknys, A.; Tornau, E. E. Transition order and dynamics of a model with competing exchange and dipolar interactions. *J. Magn. Magn. Mater.* **2009**, *321*, 137–143.

(25) Ibenskas, A.; Tornau, E. E. Statistical model for self-assembly of trimesic acid molecules into homologous series of flower phases. *Phys. Rev. E* **2012**, *86*, 051118.

(26) Misinas, T.; Tornau, E. E. Ordered assemblies of triangular-shaped molecules with strongly interacting vertices: Phase diagrams for honeycomb and zigzag structures on triangular lattice. *J. Phys. Chem. B* **2012**, *116*, 2472–2482.

(27) Ibenskas, A.; Simenas, M.; Tornau, E. E. Numerical engineering of molecular self-assemblies in a binary system of trimesic and benzenetribenzoic acids. *J. Phys. Chem. C* **2016**, *120*, 6669–6680.

(28) Ibenskas, A.; Šimėnas, M.; Tornau, E. E. A three-dimensional model for planar assembly of triangular molecules: Effect of substrate-molecule Interaction. *J. Phys. Chem. C* **2017**, *121*, 3469–3478.

(29) Filimonov, S.; Hervieu, Y. Y. On the influence of transitions between distinct adsorption states on the desorption kinetics of molecules. *Russian Physics Journal* **2016**, 1–6.

(30) Landau, K., D.; Binder *A guide to Monte Carlo simulations in statistical physics*; Cambridge University Press: Cambridge, 2000.

# TOC Graphic

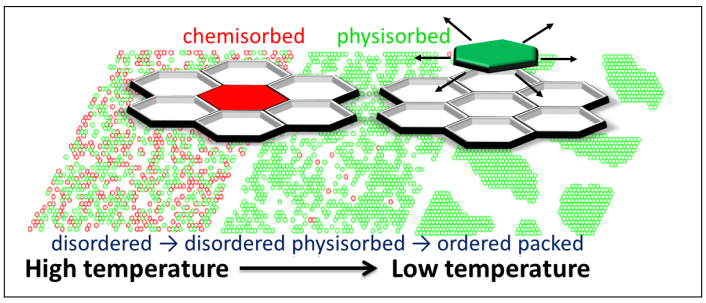
chemisorbed
physisorbed
disordered → disordered physisorbed → ordered packed
High temperature
Low temperature